Biochimica et Biophysica Acta 1798 (2010) 605–615

Contents lists available at ScienceDirect

Biochimica et Biophysica Acta

journal homepage: www.elsevier.com/locate/bbamem

Strong oligomerization behavior of PDGFβ receptor transmembrane domain and its regulation by the juxtamembrane regions

Joanne Oates, Gavin King, Ann M. Dixon *

Department of Chemistry, University of Warwick, Coventry, CV4 7AL, UK

ARTICLE INFO

Article history:
Received 15 September 2009
Received in revised form 9 December 2009
Accepted 21 December 2009
Available online 28 December 2009

Keywords:
Platelet-derived growth factor receptor
Transmembrane domain
Juxtamembrane domain
Analytical ultracentrifugation
TOXCAT

ABSTRACT

The platelet-derived growth factor β-receptor (PDGFβR) represents an important subclass of receptor tyrosine kinase (RTK) thought to be activated by ligand-induced dimerization. Interestingly, the receptor is also activated by the bovine papillomavirus E5 oncoprotein, an interaction involving the transmembrane domains of both proteins and resulting in constitutive downstream signalling. This unique mode of activation along with emerging data for other RTKs raises important questions about the role of the PDGFβR transmembrane domain in signalling. To address this, we have investigated the murine PDGFβR transmembrane and juxtamembrane domains. We show for the first time the strong oligomerization behavior of PDGFβR transmembrane domain, forming dimers and trimers in natural membranes and detergents; and that these self-interactions are mediated by a leucine-zipper-like motif. The juxtamembrane regions are found to regulate these helix–helix interactions and select specifically for dimer formation. These data provide evidence that PDGFβR is able to form ligand-independent dimers, supporting similar observations in a number of other RTK's. A point mutant in the PDGFβR juxtamembrane domain previously shown to cause receptor activation was studied and yielded no change in oligomerization or folding, suggesting (in-line with observations of the c-Kit receptor) that it may moderate interactions with other regions of PDGFβR.

1. Introduction

Receptor tyrosine kinases (RTKs) represent a large family of membrane proteins that play critical roles in many cellular processes. Activation of RTKs has been widely thought to occur via ligand binding in the extra-cellular N-terminal domain which leads to receptor dimerization. Upon dimer formation, the intra-cellular C-terminal kinase domains are brought into close proximity in the proper orientation enabling autophosphorylation and leading to activation of downstream signalling cascades (reviewed in [1]). However, recent studies of RTKs suggest that, instead of causing receptor dimerization, ligand binding may simply stabilize a particular dimeric conformation of the receptor, therefore shifting the equilibrium towards an active conformation (discussed in [2]). In a number of cases, RTKs have been shown to exist as ligand-independent inactive dimers or tetramers, which undergo a conformational change upon ligand binding [3,4]. In either case, RTK activation involves the transmission of information from the extra-cellular ligand binding domain to the intra-cellular signalling domain. This suggests a possible role for the transmembrane (TM) domain in the formation of active receptor complexes and indeed this has been demonstrated in an increasing number of receptor subclasses [2,5,6]. Further investigations involving the study of this key region of RTKs will undoubtedly increase our understanding of these important receptors.

The platelet-derived growth factor β receptor (PDGFβR) is a type III RTK with functions in cell growth, shape, and chemotaxis [7,8]. A fundamental role for the TM domain of PDGFβR in receptor activation is demonstrated by its productive interaction with E5, a small viral oncoprotein from *bovine papillomavirus* [9–11]. E5 is able to bind and activate the receptor without any involvement from the ligand binding region [12–15] and residues within the TM domains of both proteins have been shown to be critical for activation [16–20]. It is thought that an E5 homodimer is able to recruit two PDGFβR monomers resulting in an E5-stabilized dimeric receptor [21]. However, the mechanistic details of this process are unknown. Using the rationale above, E5 binding could also trigger a conformational change in a pre-formed PDGFβR dimer, preferentially stabilizing the active state. At present there is no evidence for the formation of inactive PDGFβR dimers.

Previous studies of PDGFβR have centered on the soluble regions of the protein. The structure of the extra-cellular domain has been well studied [22,23]; and a crystal structure of the closely-related stem cell factor (c-Kit) receptor N-terminal domain is also available [24]. The juxtamembrane (JM) region has been shown to have an important function in both PDGFβR and c-Kit, with mutations in the former leading to constitutive receptor activation [25,26] and mutations in the latter leading to a number of tumours [27,28].

* Corresponding author. Tel.: +44 24761 50037; fax: +44 24765 24112.
E-mail address: ann.dixon@warwick.ac.uk (A.M. Dixon).

0005-2736/$ – see front matter
doi:10.1016/j.bbamem.2009.12.016

Studies of the PDGFβ receptor TM domain however have focussed primarily on the interaction with E5, with few studies exploring the homo-oligomerization behavior of the TM domain in detail [12,13]. Understanding the role of the TM domain will have significant implications in uncovering the molecular mechanism of receptor activation both for PDGFβR and RTK's in general.

Here we address these issues though a detailed investigation of the murine PDGFβR TM and JM domains. We detect strong self-association of the TM domain, which appears to form both dimers and trimers in vitro, and describe a possible role for a leucine-zipper-like motif in this self-association. We show that the strong oligomerization of the TM domain is moderated by the JM regions of the protein. A point mutant in the PDGFβR JM domain (V536A) previously shown to cause receptor activation [25] was also studied and yielded no changes in either receptor oligomerization or protein fold, and may lead to receptor activation via changes in interactions with other proteins or with other regions of the PDGFβ receptor.

2. Materials and methods

2.1. TOXCAT in vivo oligomerization assay

To probe the propensity of the TM domain of PDGFβR to oligomerise in vivo, the TOXCAT assay was used as described previously [29,30]. Briefly, the DNA sequence corresponding to residues K499–W524 of the mature murine PDGFβR was cloned in to the pccKAN vector between the dimerization-dependent DNA-binding domain of ToxR, and maltose binding protein (MBP), and expressed in *Escherichia coli* cells. TM domain-driven oligomerization of the fusion protein leads to ToxR mediated activation of the reporter gene chloramphenicol acetyltransferase (CAT). The level of CAT expression is proportional to the strength of TM self-association, with data being normalized to the strongly dimeric TM domain from glycophorin A (GpA). Prior to carrying out the assay, correct membrane insertion was confirmed via protease sensitivity in a spheroplast assay [30] and comparable expression levels confirmed by immunoblotting using an antibody against MBP. The FAST CAT kit (Invitrogen) was used to perform the CAT assays according to the manufacturer's instructions. Mutagenesis was performed by Quikchange mutagenesis (Stratagene) according to manufacturer's instructions.

The resulting CAT activities were normalized for total fusion protein expression using the ImageJ program [31] to quantitatively analyze expression levels (i.e. intensities of bands) in anti-MPB western blots of each chimera. Statistical evaluation of all TOXCAT data from wt PDGFR and the various mutants was then carried out using a Student's *t*-test with four degrees of freedom ($DOF = 4$) and a probability (p) of 0.05 (95% confidence interval) to establish whether the effect of a given mutation was significant within the error.

2.2. Peptide synthesis and purification

A peptide corresponding to the TM domain of PDGFβR was synthesized at the Keck Facility (Yale University), using F-moc chemistry. The full sequence of the peptide was Ac-KFKVVVISAILALVVLTVISLII-LIMLWQKK-$CONH_2$ containing residues F498 to K527 of the mature protein with the addition of one non-native lysine residue at the N-terminus to aid solubility and end caps on the N- and C-termini. The crude peptide was purified by reverse-phase HPLC on a semi-preparative C4 column (Phenomenex) using a linear gradient of acetonitrile containing 0.1% trifluoroacetic acid (TFA) for the mobile phase. Pure fractions (95%) were confirmed by electrospray mass spectrometry, pooled and lyophilised (mass predicted = 3535 Da; mass observed = 3536. Peptide concentrations were calculated from the absorbance at 280 nm using a molar extinction coefficient (ε_{280}) of 5500 mol^{-1} cm^{-1}.

2.3. Analytical ultracentrifugation

The PDGFβR TM domain peptide was prepared in 50 mM Tris buffer (pH 7.5), containing 15 mM dodecylphosphocholine (DPC) (Avanti Polar Lipids, Alabaster AL, USA), 100 mM NaCl, and 52.5% D_2O (Cambridge Isotope Laboratories, Andover MA, USA) to match the buoyant density of the detergent. Sedimentation equilibrium and sedimentation velocity measurements were carried out and analyzed as described previously [32]. Briefly, sedimentation velocity data were recorded at a speed of 40,000 RPM and a temperature of 20 °C using a double-channel centerpiece, interference optics, and peptide concentrations of 96 μM and 48 μM. The resulting data profiles were fit using the program Sedfit [33] to generate a continuous sedimentation coefficient distribution, which was subsequently converted to a molecular mass distribution. Equilibrium data were recorded at 20 °C using absorbance optics set to 280 nm, a six-channel centerpiece, and peptide concentrations of 96 μM, 64 μM and 32 μM. Measurements were taken at three speeds (37,000, 40,000 and 43,000 RPM). The PDGFβR TM peptide monomeric molecular mass in 52.5% D_2O was determined to be 3.56 kDa (corrected for H–D exchange) using the program SEDNTERP (available at http://www.rasmb.bbri.org/). Global fitting of all nine data sets was carried out using a non-linear least-squares curve fitting algorithm in the program Win-NONLIN [34].

2.4. SDS-polyacrylamide gel electrophoresis (PAGE)

The PDGFβR TM peptide was prepared for electrophoresis by dissolving the required amount of peptide in 50 mM sodium phosphate buffer (pH 7.5) containing 10 mM sodium dodecyl sulphate (SDS), and 100 mM NaCl. Samples were applied to a 12% NuPAGE Bis–tris gel (Invitrogen) according to manufacturers' guidelines. Peptide visualization was achieved by staining with Coomassie-R250.

2.5. Computational searches using CHI

Structural calculations were carried out using the CNS searching of helix interactions (CHI) method [35], on an 8 node dual 2.66 GHz Xenon processor Linux cluster (Streamline computing, Warwick, UK) as described previously [29]. Both dimer and trimer models were calculated containing residues K499–W524 from the mature PDGFβR sequence. Starting geometries incorporated both left- and right-handed crossing angles of 25°; with a distance of 10.4 Å (dimer) and 11 Å (trimer) between the helices. Full searches of the dimer were carried out by rotating each helix around its central axis through 360° in 45° increments, while symmetrical searches of the trimer were conducted by rotation of the helices in 10° increments, followed by simulated annealing and energy minimization. Clusters of 10 or more structures with a backbone RMSD of ≤1 Å were created and an average structure calculated.

2.6. Cloning and expression of truncated PDGFβR and V536A mutant

Expression of the truncated PDGFβR, containing the TM domain plus 40 residues from both the C- and N-terminal JM regions, was performed as follows. The following PCR primers were used to amplify DNA corresponding to residues V460–P564 of mature PDGFβR (kindly provided by Prof. D. DiMaio, Yale University), incorporating BamH1 and Xho1 restriction sites at the 5′ and 3′ ends, respectively (underlined): forward GCATGCGATCCGTGAGCACACTGCGCCTGCGC-CACG; reverse GCATGCCTCGAGTGGCAGCTCCCAGGTGGAGTCGTAA. This was subsequently ligated into the multiple cloning site of the pET30a vector (Novagen), resulting in a construct containing a hexahistidine (His) tag at both the N- and C- termini and a linker region between the N-terminal His tag and the start of PDGFβR. The V536A mutation was constructed using the Quikchange site-directed

mutagenesis kit (Strategene) according to manufacturer's guidelines. Protein expression was carried out in the BL21 strain of *E. coli*, using 1 mM IPTG to induce expression from the T7 promoter once the culture reached mid-exponential phase. The cells were cultured for a further 4 h before being harvested by centrifugation at 3000×*g*. The resulting pellets were stored at −80 °C until required.

2.7. Purification of truncated PDGFβR protein

The truncated PDGFβR protein was directed to inclusion bodies. To isolate the protein, cell pellets were first resuspended in 5 ml Tris–acetate (pH 8.2), followed by addition of protease inhibitors (inhibitor cocktail set VII, Novagen). Lysozyme and DNase were added to final concentrations of 0.2 mg/ml and 10 μg/ml, respectively, and incubated on ice for 5 min, followed by 3×30 s sonication steps using a probe tip sonicator. Inclusion bodies were isolated by centrifugation for 90 min at 50,000×*g* in a Sorvall RC 6 Plus centrifuge. The resulting pellet was solubilized using 6 M guanidine hydrochloride in buffer containing 100 mM sodium phosphate and 10 mM Tris pH 8, for 16 h at 4 °C with gentle rotation. Insoluble material was removed by centrifugation at 50,000×*g* for 15 min. The supernatant was incubated with 1 ml of His-bind resin (Novagen) for 4 h at 4 °C. This mixture was subsequently decanted into a plastic disposable column, and the liquid drained off. The resin containing bound protein was then washed with 4 column volumes (CVs) of 8 M Urea in 100 mM sodium phosphate buffer (pH 8). Protein refolding was achieved by washing the resin with 20 CVs detergent buffer containing 0.1% n-dodecyl-β-D-maltoside (DDM) (Calbiochem), 50 mM sodium phosphate (pH 8), 300 mM sodium chloride, and 5% glycerol. Any non-specifically binding proteins were removed by washing the resin in detergent buffer containing increasing amounts of imidazole. Bound protein was eluted using 6×1/2 CV of detergent buffer containing 300 mM imidazole. Desalting and removal of imidazole was achieved using a PD10 column (Amersham) according to manufacturer's guidelines. Protein concentrations were estimated from the absorbance at 280 nm using a molar extinction coefficient (ε_{280}) of 22,460 mol^{-1} cm^{-1}.

2.8. Chemical crosslinking

Crosslinking reactions were carried out by addition of the bis (sulfosuccinimidyl) suberate (BS_3) (Pierce) crosslinker to purified protein in 0.1% DDM. The reaction was allowed to proceed for 30 min followed by subsequent addition of quencher (20 mM Tris). Crosslinked and uncrosslinked protein samples were applied to a 12% NuPAGE Bis–tris gel (Invitrogen) according to manufacturer's guidelines. Protein visualization was achieved by immunoblotting using antibodies against the C-terminal His tag (Invitrogen). The ImageJ program [31] was then used to measure the relative intensities of the bands in high-resolution images of the resulting Western blots, and these intensities were used to calculate the % dimer ($\%_d$) according to the equation:

$$\%_d = \left(\frac{I_d}{I_m + I_d}\right) \times 100$$

where I_d was the intensity of the dimer band and I_m was the intensity of the monomer band.

2.9. Circular dichroism (CD)

CD measurements were carried out on a Jasco J715 or J815 spectropolarimeter, using a 1 mm path-length quartz cuvette (Starna, Optiglass Ltd). Spectra were recorded from 260 nm to 195 nm with a 2 nm bandwidth, 0.2 nm data pitch, 100 nm min^{-1} scanning speed, and a 1 s response time. For temperature controlled experiments, a Peltier thermally-controlled cuvette holder was used. Data shown were averaged from four individual spectra and measurement of the buffer without peptide was subtracted to obtain the final spectrum. Purified protein samples were measured in buffer containing 0.1% DDM, 50 mM sodium phosphate (pH 8), 100 mM sodium chloride, and 5% glycerol. The final protein concentration was 24 μM. Analysis of secondary structure content was performed using CDSSTR software [36] and the prediction program PROFsec on the PredictProtein server [37].

3. Results

3.1. Oligomerization of the TM domain of murine PDGFβR in vivo

The TM domains of a number of RTKs have been shown to play a central role in receptor activation and signal transduction (reviewed in [2]). However, there are currently no data for the TM domain of PDGFβR, or any other type III RTK. The ability of the PDGFβR TM domain to oligomerize in natural membranes (specifically, the inner membrane of *E. coli*) was determined here using the TOXCAT assay [30]. This assay has been used to define the oligomerization behavior of a number of TM domains including those from other RTKs [6,29,38,39]. The amino acid sequence of the predicted TM domain of the murine PDGFβ receptor (Fig. 1A) was expressed as a fusion protein containing an N-terminal ToxR DNA-binding domain and maltose binding protein at the C-terminus. In the TOXCAT assay, oligomerization of the TM domain leads to ToxR dimerization, and expression of the reporter protein chloramphenicol acetyl transferase (CAT). Reporter activity is compared to that of the strongly dimerizing TM domain from glycophorin A (GpA) [40] and a dimerization-defective mutant of GpA (G83I). The results are presented in Fig. 1B, after normalization of the data for expression level (see Materials and methods), where high CAT activity was observed for the PDGFβR TM domain. The data for the wt PDGFβR TM domain and that of

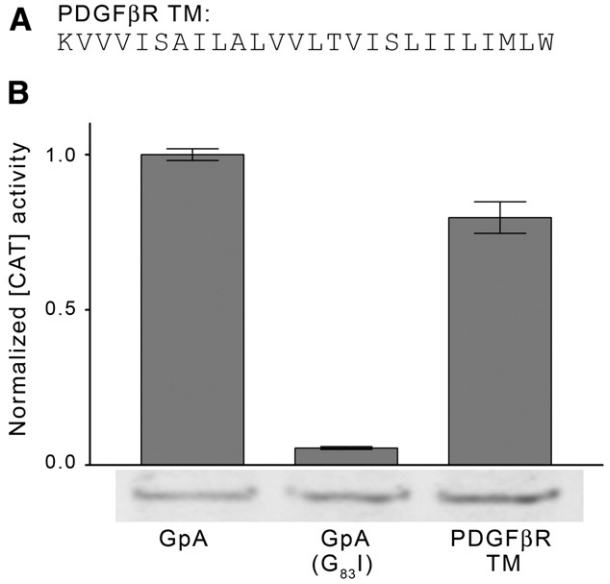

Fig. 1. Oligomerization of PDGFβR TM domain in *E. coli* membranes. (A) Sequence of PDGFβR transmembrane domain analyzed using the TOXCAT assay (residues K499–W524). (B) Results of TOXCAT assay showing CAT activities obtained for the positive and negative controls, namely the TM domain of glycophorin A (GpA) and its dimerization-defective mutant G83I, along with the PDGFβR TM domain. CAT activities are means (after normalization to fusion protein concentration, and then to the value for GpA) of three or more independent measurements +/− the standard error of the mean (SE). Western blots against maltose binding protein (MBP) are shown below the TOXCAT data to confirm expression levels of each fusion protein.

GpA were also compared using a Student's *t*-test (*DOF* = 4; $p = 0.05$; see Materials and methods). This analysis indicated that there was no significant difference between the signals of PDGFβR and GpA, demonstrating the intrinsic ability of the PDGFβR TM domain to mediate oligomerization in a natural membrane environment.

3.2. Mutagenic strategies to locate regions of the TM domain that mediate oligomerization

To investigate which residues or sequence motifs are involved in oligomerization of the TM domain, a site-directed mutagenesis approach was used. Firstly, since TM domain interaction with the BPV E5 protein leads to receptor activation, we proposed that residues known to be involved in the interaction with E5 would not be involved in homo-oligomerization of PDGFβR. Specifically, K499 in the PDGFβR TM domain is predicted to interact with D33 of E5 while T513 is expected to form a hydrogen bond to Q17 of E5 [19]. In our experiments, both of these residues were replaced with alanine as it is neither charged nor capable of hydrogen bond formation (Fig. 2A); the resulting CAT activities are shown in Fig. 2B. Comparison of the data obtained for the wt PDGFβR TM domain with these two mutants using a Student's *t*-test (*DOF* = 4; $p = 0.05$) indicates that the differences in the data resulting from either mutation are not statistically significant, and suggests that neither of these mutations significantly altered the oligomerization behavior of the TM domain. Thus we can conclude that the E5 binding interface is not involved in PDGFβR homo-oligomerization. This is not surprising given that residues known to interact with E5 are likely to be accessible and not participating in other interactions.

Apart from residues that contribute to productive interaction with E5, there is very little known about the role of individual residues in the PDGFβR TM domain. To address this we initially chose to apply a coarse systematic approach to broadly locate regions of the TM domain which affect oligomerization. This was performed by the successive replacement of groups of five consecutive residues with five alanine residues along the length of the TM domain to generate five poly-alanine mutants (Ala 1–Ala 5, moving from the N- to the C-terminus; Fig. 2A). Analyses of the data shown in Fig. 2B using a Student's *t*-test (*DOF* = 4; $p = 0.05$) indicate that, with the exception of the Ala 3 mutant at the center of the TM domain, all of the remaining four poly-alanine mutations significantly alter the CAT activity as compared to wt PDGFβR. The mutants at either end of the TM domain (Ala 1 and Ala 5) greatly reduce homo-oligomerization, suggesting that these residues affect packing interactions between the helices. Only one poly-alanine mutant, Ala 2, had a positive effect on TM domain self-association. Closer examination of the sequence covered by Ala 2 reveals a small–XXX–small motif (S504–XXX–A508); this type of motif is closely related to the GXXXG motif [41,42] and is believed to be involved in contributing to helix–helix interactions in other membrane proteins [6,43]. The SXXXA motif is also well conserved in other RTKs [44]. Here, however, mutation of A508 with either leucine (data not shown) or tryptophan (Fig. 2C–D) resulted in no significant change (as evaluated by Student's *t*-test) in the observed CAT activity as compared to wild-type. It therefore seems unlikely that this motif is significantly contributing to oligomerization; however given that the results from alanine scanning mutagenesis show a marked increase in oligomerization propensity in this region, small residues are clearly favourable at these positions.

To look for a possible interaction interface, we undertook tryptophan scanning mutagenesis in the central region of the TM domain, covering each face of the helix from A508 to T513. This type of mutagenesis has been applied successfully in previous studies where placing a tryptophan residue at the interface was presumed to disrupt oligomerization [45,46], however the converse has also been reported [47]. Therefore, for the Trp point mutants, we simply looked for

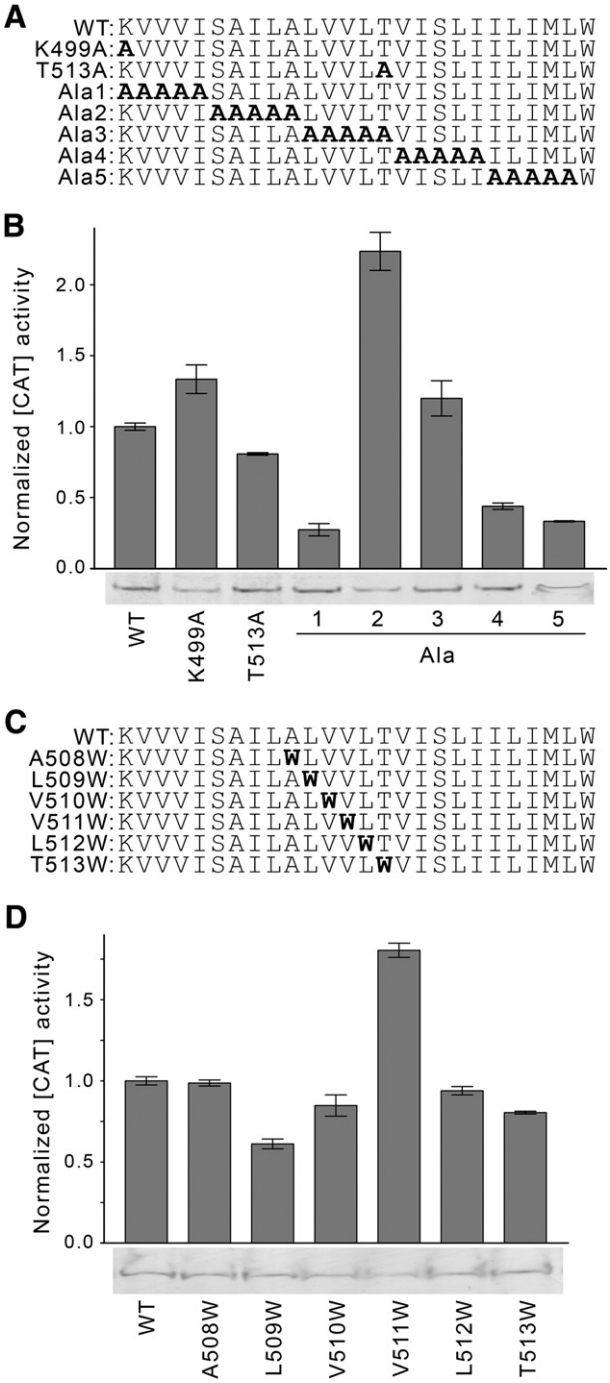

Fig. 2. TOXCAT analyses of PDGFβR TM domain mutants. (A) Amino acid sequences of the wild-type (WT) PDGFβR TM domain, point mutants K499A and T513A, and the poly-alanine mutants. (B) CAT activities obtained from the TOXCAT assay using these sequences. (C) Amino acid sequences of wt PDGFβR TM domain and the various tryptophan point mutants. (D) Resulting CAT activities obtained from these sequences. In both cases, CAT activities are means (after normalization to fusion protein concentration, and then to the value for wt PDGFβR) of three or more independent measurements +/− the standard error of the mean (SE). Western blots against maltose binding protein (MBP) are shown below the TOXCAT data to confirm expression levels of each fusion protein.

changes (positive or negative) in CAT activity. The results presented in Fig. 2D demonstrate a significant change (as evaluated by Student's *t*-test) in CAT activity upon mutation of two positions: L509, and V511. For both mutants, an apparent increase in oligomerization is observed. Plotting these residues on a helical wheel for a left-handed coiled-coil (as shown in Fig. 3A and previously in [19]) places them on

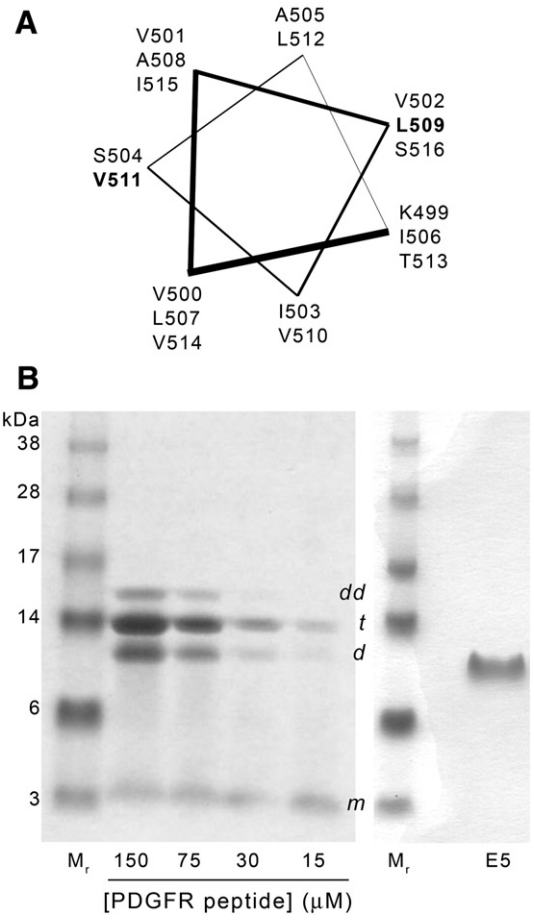

Fig. 3. Helical wheel and SDS-PAGE analyses of the PDGFβR TM domain. (A) The PDGFβR TM domain sequence plotted on a helical wheel plot for a left-handed coiled-coil. The positions shown to produce large changes in the Trp scan are shown in bold. (B) (left panel) SDS-PAGE analyses of a synthetic peptide corresponding to the TM domain of PDGFβR. Purified peptide was dissolved in buffer containing 10 mM SDS to give final peptide concentrations between 15 and 150 μM. Peptide visualization was achieved by staining with Coomassie-R250. Molecular weight markers are shown in the left-hand lane. Oligomeric states are indicated on the right (m = monomer, d = dimer, t = trimer, dd = dimer of dimers or tetramer). (right panel) Similar SDS-PAGE analysis of a peptide containing the TM domain of the E5 protein. Comparison of the migration pattern of the E5 TM peptide, which is approximately the same mass and known to form a strong dimer [32]), to that of the PDGFβR TM peptide suggests that the PDGFβR band labelled d is most likely a dimer.

different faces of the α-helix. Therefore, while it is impossible to say from this data alone what effects the Trp residues have on structure, the data suggest at a minimum that more than one interface may be involved in the interaction and/or more than one oligomeric state may be present in the membrane.

3.3. PDGFβR TM domain peptide can form dimeric and trimeric complexes in vitro

Since the TOXCAT assay cannot report on the order of the oligomers formed in the membrane, the oligomeric state of the PDGFβR TM domain was studied using a synthetic peptide containing residues F498 to K527 of the full-length protein (see Materials and methods for sequence). The purified peptide was analyzed by SDS-PAGE and visualized by staining with Coomassie R-250. Fig. 3B shows the migration pattern produced by four different concentrations of the peptide. Four distinct bands are present on the gel which we initially assumed represent the monomer, dimer, trimer and tetramer (or dimer of dimers) states. It is clear from this result that the TM domain is forming SDS-stable homo-oligomeric complexes, in good agreement with our observations in natural membranes using the TOXCAT assay (see above). SDS-stable TM domain oligomers are not uncommon in the literature [32,40], although recent reports urge caution when interpreting results from SDS-PAGE because, in some cases, slower migration is caused by differential detergent binding rather than oligomerization [48,49]. Here a monomer band is clearly present at the correct molecular weight (3.5 kDa, labelled m in Fig. 3B) and therefore it can be concluded that the other three bands represent higher-order oligomeric species. However, the oligomer bands are migrating slightly slower than would be expected from the calculated molecular weight of the peptide dimer (7 kDa), trimer (10.6 kDa), and tetramer (14.1 kDa). The position of the dimer band (labelled d in Fig. 3B) is very similar to that from another strongly dimeric TM domain peptide of approximately the same mass (the TM domain of the E5 protein, see Fig. 3B, right panel [32]), indicating that this band is most likely a PDGFβR dimer. The most intense band on the gel is directly above the dimer band, and we have provisionally assigned that to the trimeric species. Finally, the highest band on the gel (and the weakest of the oligomer bands) has been assigned to tetramer (or a dimer of dimers). Thus, our analyses suggest that the PDGFβR TM domain migrates predominantly as dimers and trimers on SDS-PAGE gels, with some tetramer formation at the highest peptide concentrations.

In order to determine more accurately the oligomeric state(s) adopted by the PDGFβR TM domain peptide, we carried out analytical ultracentrifugation (AUC) studies using the less-denaturing detergent dodecyl phosphocholine (DPC). AUC is a powerful technique well-suited to investigation of membrane protein complexes, as comparison to standards is not required and thermodynamic parameters can be obtained. Firstly, sedimentation velocity experiments were carried out at two different peptide concentrations (both solubilized in

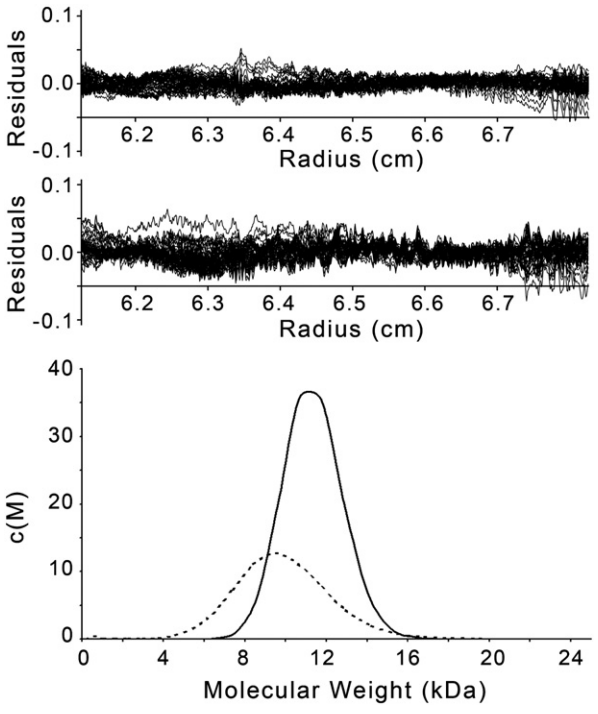

Fig. 4. Sedimentation velocity analysis of the PDGFβR TM domain. The PDGFβR peptide was prepared in 15 mM DPC as described in Materials and methods and sedimentation velocity data were collected using a double-channel centerpiece and a speed of 40K RPM. Data obtained at two different peptide concentrations (96 and 48 μM) were analyzed using the program Sedfit [33]. The molar mass distribution from the 96 μM (solid line) and 48 μM (dotted line) samples are shown, and the peak maxima correspond to masses of 11.7 and 9.5 kDa, respectively. The fit residuals at each concentration are shown in the upper plots.

15 mM DPC). The fit data and fit residuals are shown in Fig. 4. The final root mean squared deviations (RMSDs) for the fitting were 1.3×10^{-2} and 1.2×10^{-2} for the 94 μM and 48 μM samples, respectively. In the sample containing 94 μM peptide, the mass distribution profile gives a peak molecular weight of 11.7 kDa, which is just above the calculated mass of the trimeric species (10.7 kDa, accounting for H/D exchange in 52.5% D_2O). Given the relative broadness of the peak, a contribution from other oligomeric complexes is very likely; the small difference in size between dimer and trimer for example would be very difficult to resolve. Interestingly, the peak position is slightly shifted towards lower molecular weight species in the lower concentration sample (48 μM) yielding a peak molecular weight of 9.5 kDa, lying between the dimer and trimer molecular weights.

To complement these data, and to obtain thermodynamic information about the interaction, sedimentation equilibrium experiments were carried out. Global analyses were performed on data sets obtained for three peptide concentrations (from 32 to 96 μM) at three different speeds (37,000, 40,000 and 43,000 RPM), using a non-linear least-squares fitting procedure. Initial fitting to an ideal single species model yielded a mass value closely corresponding to that of the trimer, which is in good agreement with the velocity and electrophoresis data and indicates that the majority of the peptide is in a trimeric state. Fitting to various simple monomer/*n*-mer equilibria suggested that a monomer/trimer model best described the data (as judged by the randomness of the fit residuals and the minimization of the square root of variance (SRV), see Table 1). Interestingly, the addition of a dimeric species into the monomer/trimer model further improved the fit (Table 1). To obtain realistic values for the association constant, a non-ideality term (in best fit, $B=-0.0364$; see Fig. 5) was also included in the fitting process. Non-ideal behavior in these types of associating systems has been observed and discussed previously [32]. The resulting global fit of the data to a monomer/dimer/trimer equilibrium, as well as the fit residuals, are shown in Fig. 5. Analysis of the fit yielded apparent monomer/dimer and monomer/trimer dissociation constants ($K_{d,app}$) of 500 μM and 24 nM, respectively. These values were converted to apparent free energies of dissociation $\Delta G_{app}=4.4$ kcal mol^{-1} for the dimer and 10.2 kcal mol^{-1} for the trimer at 20 °C. To facilitate comparison of this value to other published data and take into account detergent concentration, ΔG_{app} was then converted to a mole fraction standard state free energy of dissociation as described previously [32,50]. This conversion resulted in free energies of dissociation of 2.0 kcal mol^{-1} for the PDGFβR TM dimer and 7.8 kcal mol^{-1} for the PDGFβR TM trimer (as compared to 7.0 kcal mol^{-1} for the GpA TM dimer [50] and 5.0 kcal mol^{-1} for the E5 TM dimer [32]).

These data demonstrate that in isolation the PDGFβR TM domain forms a very strong trimer and a more weakly-associating dimer. Interestingly, although there are no previous data to suggest that full-length PDGFβR can form a trimer in vivo, the TM domains of the ErbB family of RTKs have also been observed to form trimers in AUC experiments [51].

Table 1
Non-linear least-squares fitting statistics[a] for sedimentation equilibrium data and resulting dissociation constants[b] for PDGFβR TM domain.

Fit	Variance	SRS	SRV	DOF	K_d (M) dimer	K_d (M) trimer
M	2.94×10^{-4}	0.17	1.72×10^{-2}	561	–	–
M/D	1.15×10^{-2}	6.45	1.07×10^{-1}	561	–	–
M/Tr	7.53×10^{-5}	0.042	8.67×10^{-3}	561	–	2.68×10^{-8}
M/Tet	9.02×10^{-5}	0.051	9.50×10^{-3}	561	–	–
M/D/Tr	7.39×10^{-5}	0.042	8.60×10^{-3}	561	5.0×10^{-4}	2.39×10^{-8}

[a] Statistics are given for fits to monomer (M), monomer–dimer (M/D), monomer–trimer (M/Tr), monomer–tetramer (M/Tet) and monomer–dimer–trimer (M/D/Tr) equilibria. Variance of fit, sum of residuals squared (SRS), square root of variance (SRV), and the number of degrees of freedom in the fit (DOF) are shown.

[b] Also shown are the apparent dissociation constants (K_d) as calculated from the fits for both dimer and trimer.

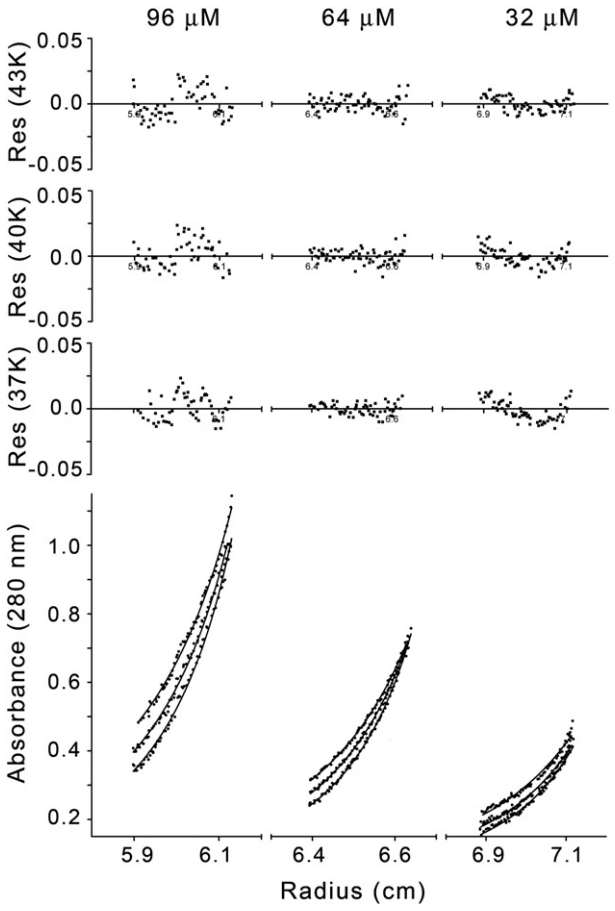

Fig. 5. Sedimentation equilibrium analysis of the PDGFβR TM domain. Global analysis of three concentrations of the PDGFβR peptide ranging from 96 to 32 μM, at three separate speeds (37K, 40K, and 43K RPM), is shown in the lower panel. In all samples, peptide was dissolved in 15 mM DPC detergent. Filled circles represent experimental data, and solid curves display the best fit resulting from the global analysis of all nine datasets, in this case a monomer–dimer–trimer model. The residuals of the fitting process at each speed are shown in the upper panels.

3.4. Structural models and mutagenesis of PDGFβR TM domain indicate a leucine-zipper-like motif stabilizes oligomer formation

In order to identify helix–helix interactions capable of stabilizing dimer and trimer formation, molecular modelling was carried out using the program CHI (see Materials and methods for details). Symmetrical left-handed coiled-coil geometries were selected based on previous studies of the PDGFβR TM domain by Petti et al. [19]. Representative structures emerged through multiple searches of both oligomeric states. The residues lying at the protein–protein interface (which were very similar in all structures obtained) are highlighted in both the TM domain sequence and the structural models of the dimer (Fig. 6 A–B) and the trimer (Fig. 6 C–D). CHI was also used to predict the energetic contribution of each amino acid to helix–helix interactions, and the resulting plots of the interaction energies for the dimer and trimer models are shown in Fig. 6E. From these data it is interesting (but not surprising) to note that the interaction 'peaks' are broader in some cases for the trimer, with two consecutive residues yielding significant interactions energies and indicating that more than one interaction interface is present.

Aside from this difference, the CHI-predicted interfaces for both the dimer and the trimer are very similar, particularly towards the C-terminus of the TM domain, and suggest that the TM domain self-associates via knobs-into-holes (or leucine-zipper) packing [52,53]. In a leucine-zipper, the interacting amino acids form a repeating motif (a heptad repeat) consisting of seven residues (*a*–*g*). Non-

polar/branched residues such as Leu and Ile usually occupy positions *a* and *d* of the heptad repeat, and these positions have been labelled beneath the PDGFβR TM domain sequence in Fig. 6A and C. For both oligomers in Fig. 6E, it can be seen that residues A505, L509, L512, S516, I519, and L523 occupy the *a* and *d* sites. Apart from A505 and S516, these residues are exactly in keeping with what is expected for a heptad repeat in an α-helical coiled-coil. In order to experimentally test whether or not these residues pack in a natural membrane bilayer, we created three mutants along the predicted leucine-zipper interface replacing small residues with Leu (A505L, S516L) or large residues with Ala (I519A) as shown in Fig. 7A. We then tested the effects of each point mutation using the TOXCAT assay (Fig. 7B).

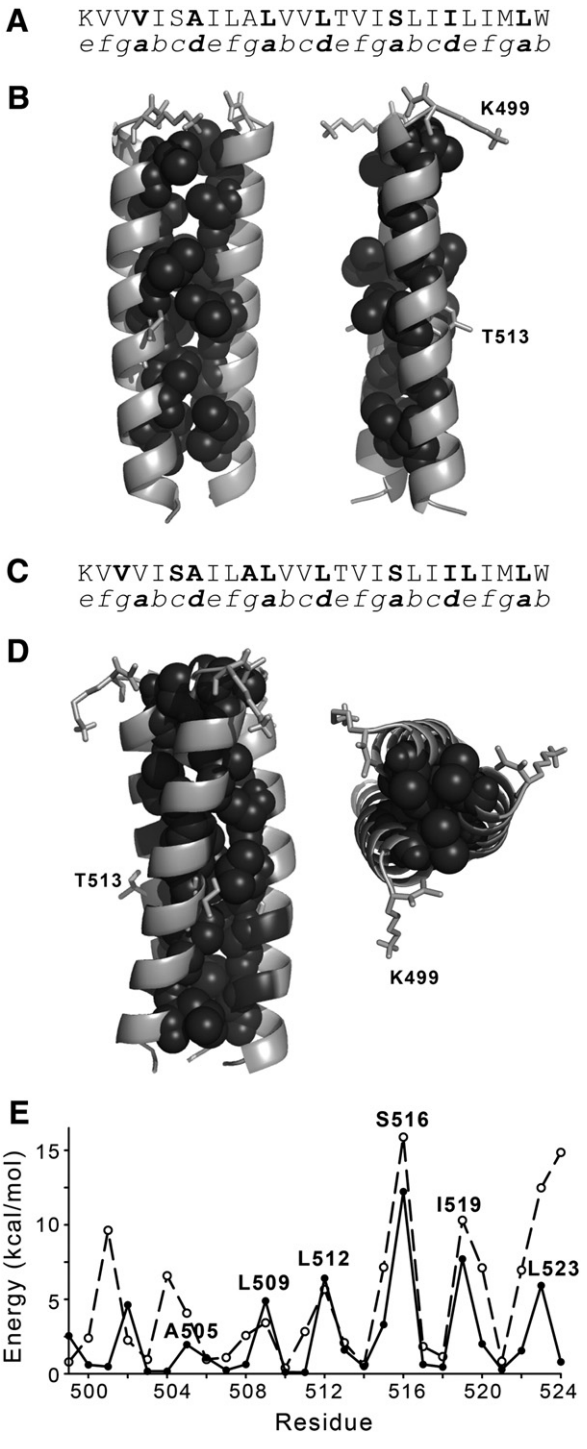

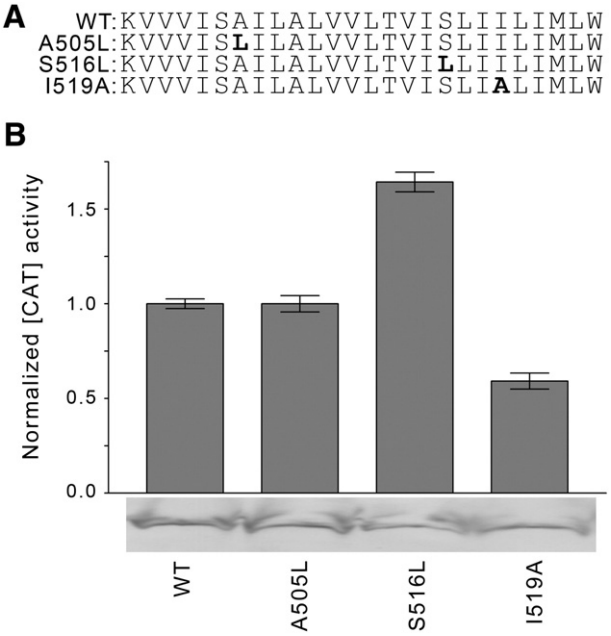

Fig. 7. Mutation of the proposed PDGFβR TM domain leucine-zipper-like interface. (A) Amino acid sequences of the wild-type (wt) PDGFβR TM domain, and point mutants of residues thought to lie on the leucine-zipper-like interface (depicted in Fig. 6). (B) CAT activities obtained from the TOXCAT assay using these sequences. CAT activities are means (after normalization to fusion protein concentration, and then to the value for wt PDGFβR) of three or more independent measurements +/− the standard error of the mean (SE). Western blots against maltose binding protein (MBP) are shown below the TOXCAT data to confirm expression levels of each fusion protein.

Although mutation of A505L had no significant effect on helix–helix association in TOXCAT, analysis of the data using a Student's *t*-test ($DOF = 4$; $p = 0.05$; see Materials and methods) indicates that replacing S516 with Leu significantly increases self-association. This result supports our theory that the TM domain self-associates via a leucine-zipper motif, as populating the *a* and *d* positions with Leu and Ile should strengthen this interaction. Conversely, we also tested the effect of removing an interfacial Ile residue (I519, predicted to lie at position *d* in the heptad repeat) with an Ala residue in an attempt to destabilize helix–helix interactions. As shown in Fig. 7B, this mutation does indeed produce a statistically significantly decrease in self-association (as indicated by *t*-test), further strengthening the argument that the *a* and *d* positions show a clear preference for branched amino acids as predicted for a leucine-zipper.

Finally, shown in Fig. 6B and 6D are the relative positions of the K499 and T513 residues in the dimer and the trimer models. In the

Fig. 6. Computational models of PDGFβR TM domain dimers and trimers. Molecular models were created using the program CHI as described in Materials and methods. (A) The sequence of the murine PDGFβR TM domain, with residues falling on the dimer interface shown in bold. Beneath the sequence is the general notation for a heptad repeat motif, identifying the position of the interfacial residues within the motif. In this arrangement, all of the interfacial residues are located at the critical *a* and *d* positions (shown in bold). (B) Front and side views of a representative left-handed dimer model, with individual helices represented as ribbons and residues lining the interface depicted as space-filling spheres. These models highlight the close packing of interfacial residues and the orientation of K499 and T513 (shown in stick representation) away from the dimer interface. (C) Positions of the residues falling on the PDGFβR TM domain trimer interface (shown in bold), and their location at positions *a* and *d* of the heptad repeat motif. (D) Side and top-views of a representative left-handed trimer model, again illustrating the packing of interfacial residues and accessibility of K499 and T513. (E) Plot of the predicted interaction energy contribution from each amino acid along the TM domain sequence (K499–W524) in the dimer (solid line) and the trimer (dashed line) models. The 'peaks' represent the residues that are found at a helix–helix interface, and these are also listed above the peak maxima. For the trimer, when more than one residue was found at an interface the peaks were slightly broadened.

models, we see that these two residues (which TOXCAT data suggest are not involved in oligomerization; see Fig. 2B) are oriented away from the dimer and trimer interfaces. As mentioned above, these residues are thought to participate in the binding of the BPV E5 protein [19] and should therefore be accessible, which is indeed what is observed in both models.

3.5. The juxtamembrane regions of PDGFβR regulate transmembrane helix–helix interactions

The strong self-association of the TM domain is surprising given the lack of evidence supporting oligomerization of the full-length protein (in the absence of ligand or the E5 protein) or any biological relevance of a trimeric state. This may suggest that regions outside of the TM domain play a role in regulating the TM helix–helix interactions. Indeed, mutations in the cytoplasmic JM region of PDGFβR and the related c-Kit receptor have been shown to lead to ligand-independent activation [25,27,54], while the extra-cellular JM domain of the Erythropoietin receptor (EpoR) is known to have a controlling role in receptor function [55]. To investigate a role for the PDGFβR JM regions in regulating TM domain oligomerization, we expressed (in *E. coli*) and purified a truncated receptor containing the TM domain, 40 residues of the N-terminal JM region, and the C-terminal JM region previously investigated by Irusta et al. [26]. The resulting protein was 105 residues in length, and contained residues V460–P564. The oligomeric state of this construct was assessed by SDS-PAGE (Fig. 8A, lane i) and immunoblotting to a His_6 Tag incorporated on the C-terminus. Two bands are observed on the blot, corresponding to the molecular weights of monomer and dimer (*m* and *d*, respectively). The dimeric state was further stabilized by the addition of the crosslinking reagent Bis [sulfosuccinimidyl] suberate (or BS_3) to protein solubilized in 0.1% n-Dodecyl-β-D-Maltoside (DDM) prior to analysis by SDS-PAGE, as shown in Fig. 8A, lane ii. In comparison to the TM domain in isolation, the longer protein contains a larger population of monomers in the presence of SDS. However, a significant amount of SDS-stable dimer can be detected and this is increased when the dimer is stabilized first by crosslinking in the less-denaturing DDM detergent. Quantification of the relative amounts of monomer and dimer (see Materials and methods) resulted in values of 4.8% dimer in the absence of crosslinker, and 21.97% dimer in the presence of crosslinker. This ~4-fold increase in the percentage dimer upon addition of crosslinker suggests that the dimeric state is stabilized by crosslinking. Even more interesting is the fact that, apart from the dimer band, we saw no evidence for any higher molecular weight species in any of the Western blots. The trimer species which was identified (together with the dimer) in the SDS-PAGE and AUC analyses of the TM domain in isolation has been eliminated in the presence of the C- and N-terminal JM domains, leaving only the more biologically-relevant dimer species.

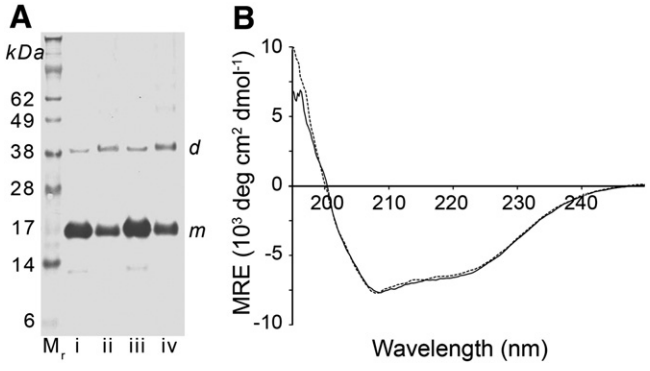

Fig. 8. PDGFβR juxtamembrane (JM) regions control TM domain association. (A) SDS-PAGE analysis of a purified, truncated PDGFβR protein containing the wt TM domain and C- and N-terminal JM regions (residues V460 to P564). Samples were analyzed both without (lane i) and with (lane ii) addition of the crosslinker BS_3. A construct containing an activating point mutation in the C-terminal JM region (V536A) was also purified and analyzed using SDS-PAGE, again in the absence (lane iii) and presence (lane iv) of BS_3. Molecular weight markers are included in the far left lane, and the oligomeric state is indicated on the right (*m* = monomer, *d* = dimer). Quantification of the resulting bands (see Materials and methods) yielded values of 4.8 and 6.5% dimer in the absence of crosslinker for wt and V536A mutant, respectively, and 21.9 and 23.7% dimer in the presence of crosslinker. (B) Circular dichroism spectra of purified wild-type (solid line) and V536A mutant (dotted line) proteins in buffer containing 0.1% dodecyl maltoside (DDM). The resulting spectra were analyzed for secondary structure content using the CDSSTR software, and both analyses produced α-helical content of 15%.

3.6. An activating point mutation in the cytoplasmic JM region does not affect oligomerization or folding

The results presented above suggest that the JM regions of PDGFβR can modify the oligomerization behavior of the TM domain. A previous study of the cytoplasmic JM domain of the PDGFβR identified a single point mutation (V536A) that lead to constitutive receptor activation [25]. To investigate whether this mutation results in changes to the oligomeric state, site-directed mutagenesis was used to introduce the analogous V536A mutation into our truncated receptor followed by analysis using SDS-PAGE (as above). The results are shown in Fig. 8A (lanes iii and iv), and interestingly no changes in the relative proportion of monomer or dimer are observed for the mutant, in either the absence or presence of the BS_3 crosslinker. Quantification of the relative amounts of monomer and dimer for the V536A mutant resulted in values of 6.5% dimer in the absence of crosslinker, and 23.7% dimer in the presence of crosslinker. These values are very similar to those obtained for the wt sequence (above). Additionally, circular dichroism (CD) was used to determine the secondary structure content of both the wt and mutant constructs, thus highlighting any differences in protein fold. The resulting spectra of both proteins (Fig. 8B) are essentially identical. The CDSSTR [36] program was used to fit the CD data and calculate secondary structure content, and both wild-type and mutant spectra yielded α-helical content of 15%. Comparison of this value to that predicted from the protein sequences (using the program PROFsec on the PredictProtein [37] server) produced very close agreement, with a predicted helical content for both proteins of 14.11%. Thermal stability of the protein fold was also assessed by CD measurements between 5 and 95 °C using a Peltier temperature control unit, and again no difference between the wt and mutant were observed (data not shown).

4. Discussion

We have carried out the first detailed investigation of the TM domain from PDGFβR, a key growth factor RTK that has roles in many cellular functions. Appreciation of the importance of TM domains in mediating protein–protein interactions in the membrane has increased markedly in recent years (for review, see Ref. [56]), with the TM domains of a number of growth factor receptors reported to play key roles in receptor dimerization and subsequent activation of downstream signalling cascades [2–6]. Evidence that the PDGFβR TM domain is involved in receptor activation comes from studies of the BPV E5 protein, where constitutive receptor signalling is mediated by E5 interaction with the TM domain; however, to-date no biophysical investigations have focussed specifically on this region. Our results demonstrate that the PDGFβR TM domain has a very strong propensity to form oligomers both in a natural membrane environment and in detergent micelles (giving dissociation constants for homo-oligomerization in the nM range). This is contrary to the oligomerization behavior reported for other RTK TM domains such as the fibroblast and epidermal growth factor receptors (FGFR3 and the ErbB family), where dimerization is significantly weaker than that for

GpA [5,6]. This may reflect differences in signalling mechanism for this receptor sub-type.

The presence of a trimeric species in both SDS-PAGE and AUC analyses was unexpected, as this type of association of PDGFβR has not been observed in a biological context. However, it is not without precedent as Stanley and Fleming observed trimeric TM domains from several members of the ErbB family of receptors using these methods [51]. In the case of the ErbB TM domains, chemical cross-linking was required to visualize the dimeric and trimeric states on gels, and the observation of TM domain trimers using AUC was dependent on the detergent concentration. It was therefore hypothesized that high peptide-to-micelle ratios may be causing non-preferential association as more monomers are forced to occupy individual micelles. Conversely, the data presented here, in particular the data shown in Fig. 3B, seem to suggest that the self-association of the PDGFβR TM domain favors dimer *and* trimer formation. Over a 10-fold change in peptide concentration (15–150 μM) we detect monomer, dimer and trimer species; the only other species observed is tetramer (or dimer of dimers) at the highest concentrations. The trimer is the most prominent band detected at all concentrations. It is worth noting that the trimer state is only observed here for a short peptide in vitro (not for the longer expressed protein in vivo), and therefore this trimer species may result from an antiparallel arrangement of the TM domains that would not be possible in native membranes in vivo. So while the trimeric state of the TM domain may not be the biologically-relevant form, it provides insight into the potentially large contribution of the TM domain to ligand-independent protein self-association, perhaps helping to stabilize pre-formed, inactive receptor dimers.

Molecular modelling and mutagenesis in this study support the model that both the PDGFβR TM domain dimer and trimer are stabilized by a very similar, leucine-zipper-like motif with key residues located at the *a* and *d* positions of a heptad repeat. The presence of leucine-zippers in transmembrane regions has been explored in the literature [52,57]; and has been identified in other RTK's, including ErbB2 [58,59] and DDR1 [60]. Interestingly, replacement of the PDGFβR TM domain with that of the ErbB2 TM domain from *rat* (also called the Neu proto-oncogene) resulted in a small amount of ligand-independent signalling. This increased significantly upon replacement of the TM with the oncogenic form of Neu (containing a single Val to Glu point mutation in the TM domain), which is known to activate full-length ErbB2 by mediating TM domain dimerization [61]. From the sequence alignment of the two TM domains carried out by Petti et al. [61], the valine/glutamic acid residue would fall on the leucine-zipper interface identified here (at position L509). The interfacial motif identified here can be used as a guide for further in vivo investigations to probe TM mediated association in the full-length receptor.

We also see that the residues in the PDGFβR TM domain thought to bind to the E5 oncoprotein lie outside of both the predicted dimer and trimer interfaces, which is consistent with the current model that these residues are accessible for binding of E5 to a pre-formed (and inactive) PDGFβR dimer. E5 binding may then trigger a conformational change in the receptor, causing it to adopt its active conformation. This feasibly could occur through rotation of the helical dimer from one interface to another, causing a more substantial rearrangement of the soluble signalling domains in the full-length receptor; however, any further speculation on the molecular mechanism by which E5 causes PDGFβR activation is beyond the scope of this work.

Although TM domain dimers and trimers are both observed in this study, the trimeric form has not been observed for the full-length receptor and is therefore not likely to be the most biologically-relevant form. Indeed, by expressing a severely truncated (105 amino acid) receptor containing the TM and C- and N-terminal juxtamembrane domains, we observed that the trimeric species is eliminated entirely and only the dimer is formed. Therefore, the JM regions are clearly involved in regulating the strong TM domain interactions and guiding formation of the native oligomeric state. The observation of a dimer species also suggests that ligand-independent, pre-formed dimers may exist in vivo for the PDGFβR. The existence of unliganded dimers has been reported for a number of other RTKs such as EGFR [62], ErbB [6], EpoR [63], and a variety of other receptors (for an excellent review see ref. [2]).

Mutagenesis of the truncated receptor at position 536 (V536A), which produced constitutive activation of the PDGFβR in vivo in a previous study [25], shows no change in the propensity to form dimers nor does it show any change in the fold (as evaluated from CD data). This is surprising in that this mutant in vivo produced levels of Ba/F3 cell survival and proliferation comparable to those observed for ligand-activated PDGFβR [25]. One explanation for this result could be that the V536A mutation leads to PDGFβR activation via changes in inter- or intramolecular protein–protein interactions, and not changes in oligomeric state or secondary structure. The intra-cellular JM domain of the closely-related c-Kit receptor has been shown to have an auto-inhibitory function by inserting into the kinase-active site and preventing formation of the active conformation [64]. Similarly, the V536A mutation in PDGFβR may destabilize intramolecular auto-inhibitory interactions of the JM domain, leading to the observed constitutive receptor activation [25]. Although these data from the literature suggest a more critical role for the intra-cellular JM domain it is not clear from our results whether one or both JM regions are exerting control over the observed oligomerization behavior. Attempts to further pinpoint the required residues by expression of shorter constructs resulted in poor expression levels; thus the precise contribution of each JM domain remains unknown. Furthermore, it will be of interest to investigate the mutations presented here in the context of the full-length receptor.

In summary, we have used a wide variety of independent biochemical and biophysical methods to provide the first detailed investigation of the role of the TM domain of PDGFβR in receptor dimerization, and find that it has key features in common with several other RTKs. These features include significant TM helix–helix interactions (although in this case they are notably stronger) and oligomerization via a leucine-zipper-like packing motif. The JM domains modulate TM interactions and select for a single (dimeric) oligomeric state in addition to monomer. However it is still to be determined whether these pre-formed oligomers adopt the active or inactive conformation. The C-terminal JM domain also appears to regulate receptor activation via intra- or intermolecular protein interactions, and not changes in fold or assembly.

Acknowledgements

This work was supported by Cancer Research UK (CR-UK) grant number C21449/A6926. We thank Prof. D. DiMaio for kindly providing the plasmid containing the full-length DNA sequence of mature PDGFβR and for many helpful discussions, Prof. D.M. Engelman for providing the expression vectors and bacterial strain for the TOXCAT assay, J. Crawford for peptide synthesis, R. Parslow for assistance with analytical ultracentrifugation, and Prof. A Rodger for use of circular dichroism instrumentation. We also thank Dr. G. Warren, Dr. A Beevers, D. Patel, and A. Nilsson for careful reading of the manuscript.

References

[1] J. Schlessinger, Cell signaling by receptor tyrosine kinases, Cell 103 (2000) 211–225.
[2] E. Li, K. Hristova, Role of receptor tyrosine kinase transmembrane domains in cell signaling and human pathologies, Biochemistry 45 (2006) 6241–6251.

[3] T. Moriki, H. Maruyama, I.N. Maruyama, Activation of preformed EGF receptor dimers by ligand-induced rotation of the transmembrane domain, J. Mol. Biol. 311 (2001) 1011–1026.
[4] F.P. Ottensmeyer, D.R. Beniac, R.Z. Luo, C.C. Yip, Mechanism of transmembrane signaling: insulin binding and the insulin receptor, Biochemistry 39 (2000) 12103–12112.
[5] E. Li, M. You, K. Hristova, Sodium dodecyl sulfate-polyacrylamide gel electrophoresis and forster resonance energy transfer suggest weak interactions between fibroblast growth factor receptor 3 (FGFR3) transmembrane domains in the absence of extracellular domains and ligands, Biochemistry 44 (2005) 352–360.
[6] J.M. Mendrola, M.B. Berger, M.C. King, M.A. Lemmon, The single transmembrane domains of ErbB receptors self-associate in cell membranes, J. Biol. Chem. 277 (2002) 4704–4712.
[7] B. Westermark, L. Claesson-Welsh, C.H. Heldin, Structural and functional aspects of the receptors for platelet-derived growth factor, Prog. Growth Factor Res. 1 (1989) 253–266.
[8] C.H. Heldin, B. Westermark, Mechanism of action and in vivo role of platelet-derived growth factor, Physiol. Rev. 79 (1999) 1283–1316.
[9] L. Petti, L. Nilson, D. DiMaio, Activation of the platelet-derived growth factor receptor by the bovine papillomavirus E5 protein, EMBO J. 10 (1991) 845–855.
[10] K. Talbert-Slagle, D. DiMaio, The bovine papillomavirus E5 protein and the PDGF b receptor: it takes two to tango, Virology 384 (2009) 345–351.
[11] D. DiMaio, C.C. Lai, O. Klein, Virocrine transformation: the intersection between viral transforming proteins and cellular signal transduction pathways, Annu. Rev. Microbiol. 52 (1998) 397–421.
[12] V.M. Nappi, J.A. Schaefer, L.M. Petti, Molecular examination of the transmembrane requirements of the platelet-derived growth factor beta receptor for a productive interaction with the bovine papillomavirus E5 oncoprotein, J. Biol. Chem. 277 (2002) 47149–47159.
[13] D.A. Drummond-Barbosa, R.R. Vaillancourt, A. Kazlauskas, D. DiMaio, Ligand-independent activation of the platelet-derived growth factor beta receptor: requirements for bovine papillomavirus E5-induced mitogenic signaling, Mol. Cell Biol. 15 (1995) 2570–2581.
[14] D.J. Goldstein, T. Andresson, J.J. Sparkowski, R. Schlegel, The BPV-1 E5 protein, the 16 kDa membrane pore-forming protein and the PDGF receptor exist in a complex that is dependent on hydrophobic transmembrane interactions, EMBO J. 11 (1992) 4851–4859.
[15] L. Petti, D. DiMaio, Stable association between the bovine papillomavirus E5 transforming protein and activated platelet-derived growth factor receptor in transformed mouse cells, Proc. Natl. Acad. Sci. U. S. A. 89 (1992) 6736–6740.
[16] L.L. Freeman-Cook, A.P. Edwards, A.M. Dixon, K.E. Yates, L. Ely, D.M. Engelman, D. Dimaio, Specific locations of hydrophilic amino acids in constructed transmembrane ligands of the platelet-derived growth factor beta receptor, J. Mol. Biol. 345 (2005) 907–921.
[17] B.H. Horwitz, A. Burkhardt, R. Schlegel, D. DiMaio, 44-amino acid E5 transforming protein of bovine papillomavirus requires a hydrophobic core and specific carboxyl-terminal amino acids, Mol. Cell. Biol. 8 (1988) 4071–4078.
[18] O. Klein, G.W. Polack, T. Surti, D. Kegler-Ebo, S.O. Smith, D. DiMaio, Role of glutamine 17 of the bovine papillomavirus E5 protein in platelet-derived growth factor beta receptor activation and cell transformation, J. Virol. 72 (1998) 8921–8932.
[19] L.M. Petti, V. Reddy, S.O. Smith, D. DiMaio, Identification of amino acids in the transmembrane and juxtamembrane domains of the platelet-derived growth factor receptor required for productive interaction with the bovine papillomavirus E5 protein, J. Virol. 71 (1997) 7318–7327.
[20] L.A. Nilson, R.W. Gottlieb, G.W. Polack, D. DiMaio, Mutational analysis of the interaction between the BPV E5 transforming protein and the endogenous receptor for platelet-derived growth factor in mouse C127 cells, J. Virol. 69 (1995) 5869–5874.
[21] C.C. Lai, C. Henningson, D. DiMaio, Bovine papillomavirus E5 protein induces oligomerization and trans-phosphorylation of the platelet-derived growth factor receptor, Proc. Natl. Acad. Sci. U. S. A. 95 (1998) 15241–15246.
[22] B. Herren, B. Rooney, K.A. Weyer, N. Iberg, G. Schmid, M. Pech, Dimerization of extracellular domains of platelet-derived growth factor receptors. A revised model of receptor–ligand interaction, J. Biol. Chem. 268 (1993) 15088–15095.
[23] Y. Yang, S. Yuzawa, J. Schlessinger, Contacts between membrane proximal regions of the PDGF receptor ectodomain are required for receptor activation but not for receptor dimerization, Proc. Natl. Acad. Sci. U. S. A. 105 (2008) 7681–7686.
[24] H. Liu, X. Chen, P.J. Focia, X. He, Structural basis for stem cell factor-KIT signaling and activation of class III receptor tyrosine kinases, EMBO J. 26 (2007) 891–901.
[25] P.M. Irusta, D. DiMaio, A single amino acid substitution in a WW-like domain of diverse members of the PDGF receptor subfamily of tyrosine kinases causes constitutive receptor activation, EMBO J. 17 (1998) 6912–6923.
[26] P.M. Irusta, Y. Luo, O. Bakht, C.C. Lai, S.O. Smith, D. DiMaio, Definition of an inhibitory juxtamembrane WW-like domain in the platelet-derived growth factor beta receptor, J. Biol. Chem. 277 (2002) 38627–38634.
[27] S. Hirota, K. Isozaki, Y. Moriyama, K. Hashimoto, T. Nishida, S. Ishiguro, K. Kawano, M. Hanada, A. Kurata, M. Takeda, G. Muhammad Tunio, Y. Matsuzawa, Y. Kanakura, Y. Shinomura, Y. Kitamura, Gain-of-function mutations of c-kit in human gastrointestinal stromal tumors, Science 279 (1998) 577–580.
[28] B.J. Longley, M.J. Reguera, Y. Ma, Classes of c-KIT activating mutations: proposed mechanisms of action and implications for disease classification and therapy, Leuk. Res. 25 (2001) 571–576.
[29] Z.A. Jenei, K. Borthwick, V.A. Zammit, A.M. Dixon, Self-association of transmembrane domain (TM) 2, but not TM 1, in carnitine palmitoyltransferase 1A: role of GXXXG(A) motifs, J. Biol. Chem. 284 (2009) 6988–6997.
[30] W.P. Russ, D.M. Engelman, TOXCAT: a measure of transmembrane helix association in a biological membrane, Proc. Natl. Acad. Sci. U. S. A. 96 (1999) 863–868.
[31] M.D. Abramoff, P.J. Magelhaes, S.J. Ram, Image processing with image, J. Biophoton. Int. 11 (2004) 36–42.
[32] J. Oates, M. Hicks, T.R. Dafforn, D. DiMaio, A.M. Dixon, In vitro dimerization of the bovine papillomavirus E5 protein transmembrane domain, Biochemistry 47 (2008) 8985–8992.
[33] P. Schuck, Size distribution analysis of macromolecules by sedimentation velocity ultracentrifugation and Lamm equation modelling, Biophys. J. 78 (2000) 1606–1619.
[34] M.L. Johnson, J.J. Correia, D.A. Yphantis, H.R. Halvorson, Analysis of data from the analytical ultracentrifuge by nonlinear least-squares techniques, Biophys. J. 36 (1981) 575–588.
[35] A.T. Brunger, P.D. Adams, G.M. Clore, W.L. DeLano, P. Gros, R.W. Grosse-Kunstleve, J.S. Jiang, J. Kuszewski, M. Nilges, N.S. Pannu, R.J. Read, L.M. Rice, T. Simonson, G.L. Warren, Crystallography & NMR system: a new software suite for macromolecular structure determination, Acta Crystallogr. D Biol. Crystallogr. 54 (1998) 905–921.
[36] N. Sreerama, R.W. Woody, Estimation of protein secondary structure from circular dichroism spectra: comparison of CONTIN, SELCON, and CDSSTR methods with an expanded reference set, Anal. Biochem. 287 (2000) 252–260.
[37] B. Rost, G. Yachdav, J. Liu, The PredictProtein server, Nucleic Acids Res. 32 (2004) W321–W326.
[38] A.M. Dixon, B.J. Stanley, E.E. Matthews, J.P. Dawson, D.M. Engelman, Invariant chain transmembrane domain trimerization: a step in MHC class II assembly, Biochemistry 45 (2006) 5228–5234.
[39] G. Warren, J. Oates, C. Robinson, A.M. Dixon, Contributions of the transmembrane domain and a key acidic motif to assembly and function of the TatA complex, J. Mol. Biol. 388 (2009) 122–132.
[40] M.A. Lemmon, J.M. Flanagan, J.F. Hunt, B.D. Adair, B.J. Bormann, C.E. Dempsey, D.M. Engelman, Glycophorin A dimerization is driven by specific interactions between transmembrane alpha-helices, J. Biol. Chem. 267 (1992) 7683–7689.
[41] W.P. Russ, D.M. Engelman, The GxxxG motif: a framework for transmembrane helix–helix association, J. Mol. Biol. 296 (2000) 911–919.
[42] A. Senes, M. Gerstein, D.M. Engelman, Statistical analysis of amino acid patterns in transmembrane helices: the GxxxG motif occurs frequently and in association with beta-branched residues at neighboring positions, J. Mol. Biol. 296 (2000) 921–936.
[43] D. Schneider, D.M. Engelman, Motifs of two small residues can assist but are not sufficient to mediate transmembrane helix interactions, J. Mol. Biol. 343 (2004) 799–804.
[44] M. Sternberg, W. Gullick, A sequence motif in the transmembrane region of growth-factor receptors with tyrosine kinase-activity mediates dimerization, Prot. Eng. 3 (1990) 245–248.
[45] A. Ortiz-Acevedo, M. Melendez, A.M. Asseo, N. Biaggi, L.V. Rojas, J.A. Lasalde-Dominicci, Tryptophan scanning mutagenesis of the gammaM4 transmembrane domain of the acetylcholine receptor from Torpedo californica, J. Biol. Chem. 279 (2004) 42250–42257.
[46] L.L. Sharp, J. Zhou, D.F. Blair, Tryptophan-scanning mutagenesis of MotB, an integral membrane protein essential for flagellar rotation in Escherichia coli, Biochemistry 34 (1995) 9166–9171.
[47] A. Ridder, P. Skupjen, S. Unterreitmeier, D. Langosch, Tryptophan supports interaction of transmembrane helices, J. Mol. Biol. 354 (2005) 894–902.
[48] W.F. Walkenhorst, M. Merzlyakov, K. Hristova, W.C. Wimley, Polar residues in transmembrane helices can decrease electrophoretic mobility in polyacrylamide gels without causing helix dimerization, Biochim. Biophys. Acta-Biomembr. 1788 (2009) 1321–1331.
[49] A. Rath, M. Glibowicka, V.G. Nadeau, G. Chen, C.M. Deber, Detergent binding explains anomalous SDS-PAGE migration of membrane proteins, Proc. Natl. Acad. Sci. U. S. A. 106 (2009) 1760–1765.
[50] K. Fleming, Standardizing the free energy change of transmembrane helix–helix interactions, J. Mol. Biol. 323 (2002) 563–571.
[51] A.M. Stanley, K.G. Fleming, The transmembrane domains of ErbB receptors do not dimerize strongly in micelles, J. Mol. Biol. 347 (2005) 759–772.
[52] D. Langosch, J. Heringa, Interaction of transmembrane helices by a knobs-into-holes packing characteristic of soluble coiled coils, Proteins 31 (1998) 150–159.
[53] D.N. Woolfson, The design of coiled-coil structures and assemblies, Adv Protein Chem 70 (2005) 79–112.
[54] H. Kitayama, Y. Kanakura, T. Furitsu, T. Tsujimura, K. Oritani, H. Ikeda, H. Sugahara, H. Mitsui, Y. Kanayama, Y. Kitamura, et al., Constitutively activating mutations of c-kit receptor tyrosine kinase confer factor-independent growth and tumorigenicity of factor-dependent hematopoietic cell lines, Blood 85 (1995) 790–798.
[55] K.F. Kubatzky, W. Liu, K. Goldgraben, C. Simmerling, S.O. Smith, S.N. Constantinescu, Structural requirements of the extracellular to transmembrane domain junction for erythropoietin receptor function, J. Biol. Chem. 280 (2005) 14844–14854.
[56] K.R. Mackenzie, Folding and stability of alpha-helical integral membrane proteins, Chem. Rev. 106 (2006) 1931–1977.
[57] W. Ruan, V. Becker, U. Klingmuller, D. Langosch, The interface between self-assembling erythropoietin receptor transmembrane segments corresponds to a membrane-spanning leucine zipper, J. Biol. Chem. 279 (2004) 3273–3279.
[58] A.J. Beevers, A. Kukol, The transmembrane domain of the oncogenic mutant ErbB-2 receptor: a structure obtained from site-specific infrared dichroism and molecular dynamics, J. Mol. Biol. 361 (2006) 945–953.

[59] E.V. Bocharov, K.S. Mineev, P.E. Volynsky, Y.S. Ermolyuk, E.N. Tkach, A.G. Sobol, V.V. Chupin, M.P. Kirpichnikov, R.G. Efremov, A.S. Arseniev, Spatial structure of the dimeric transmembrane domain of the growth factor receptor ErbB2 presumably corresponding to the receptor active state, J. Biol. Chem. 283 (2008) 6950–6956.
[60] N.A. Noordeen, F. Carafoli, E. Hohenester, M.A. Horton, B. Leitinger, A transmembrane leucine zipper is required for activation of the dimeric receptor tyrosine kinase DDR1, J. Biol. Chem. 281 (2006) 22744–22751.
[61] L.M. Petti, P.M. Irusta, D. DiMaio, Oncogenic activation of the PDGF beta receptor by the transmembrane domain of p185neu*, Oncogene 16 (1998) 843–851.
[62] X. Yu, K.D. Sharma, T. Takahashi, R. Iwamoto, E. Mekada, Ligand-independent dimer formation of epidermal growth factor receptor (EGFR) is a step separable from ligand-induced EGFR signaling, Mol. Biol. Cell 13 (2002) 2547–2557.
[63] S.N. Constantinescu, T. Keren, M. Socolovsky, H. Nam, Y.I. Henis, H.F. Lodish, Ligand-independent oligomerization of cell-surface erythropoietin receptor is mediated by the transmembrane domain, Proc. Natl. Acad. Sci. 98 (2001) 4379–4384.
[64] C. Mol, D. Dougan, T. Schneider, R. Skene, M. Kraus, D. Scheibe, G. Snell, H. Zou, B. Sang, K. Wilson, Structural basis for the autoinhibition and STI-571 inhibition of c-Kit tyrosine kinase, J. Biol. Chem. 279 (2004) 31655–31663.